SUPPLEMENTARY INFORMATION

CXCR6 Is Required for Anti-tumor Efficacy of Intratumoral CD8$^+$ T Cell

Binglin Wang, Yi Wang, Xiaofan Sun, Guoliang Deng, Wei Huang, Xingxin Wu, Yanhong Gu, Zhigang Tian, Zhimin Fan, Qiang Xu*, Hongqi Chen*, Yang Sun*.

- **Supplementary Figure 1-6**

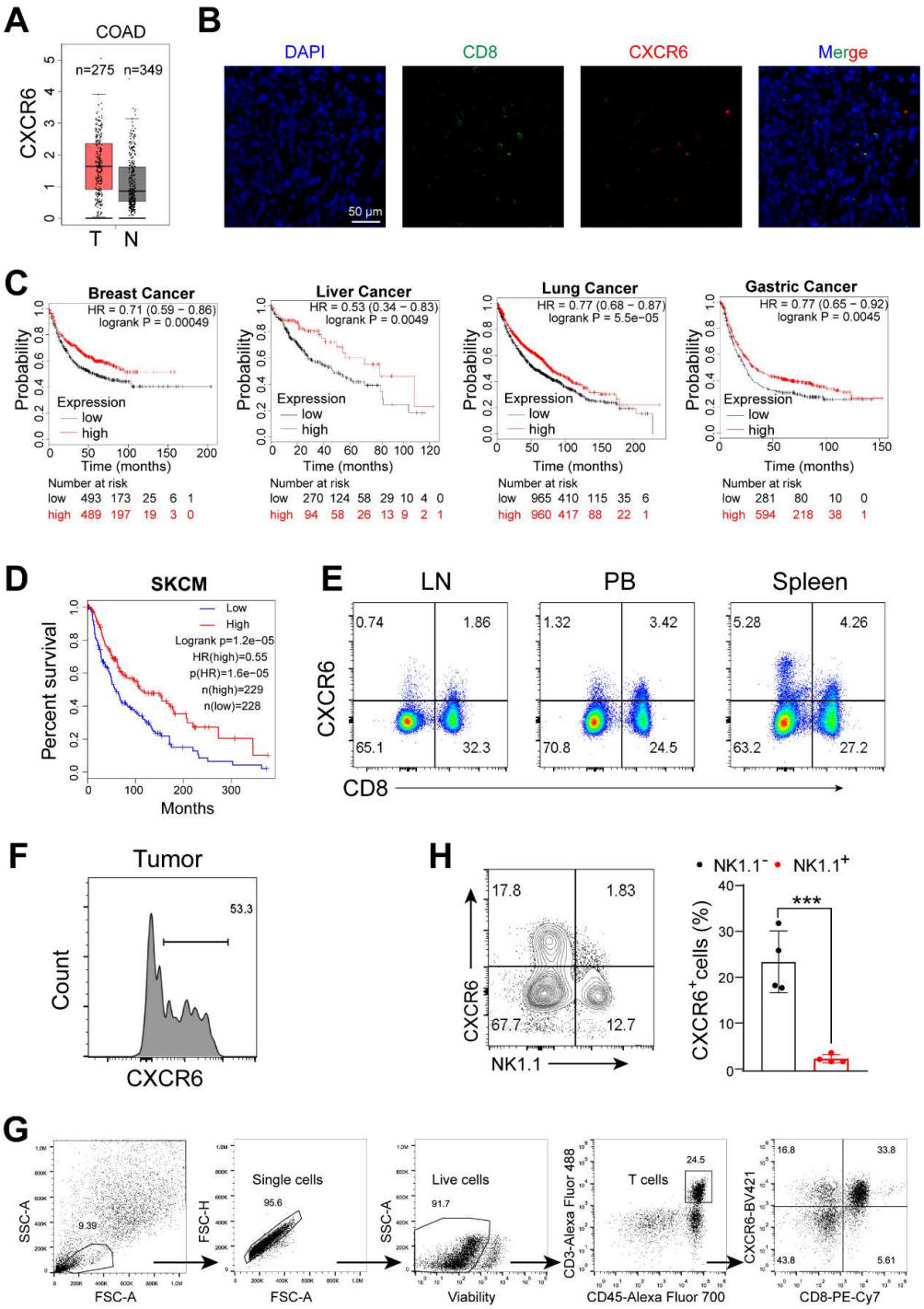

Figure S1. High expression levels of CXCR6 in tumor tissues predict good prognosis in some other cancer cohorts

A. The expression level of CXCR6 in tumor (T) and normal (N) tissues from colon adenocarcinoma (COAD) cohorts in TCGA database analyzed by GEPIA website. **B**. Immunofluorescence staining of

DAPI (blue)/CD8 (green)/CXCR6 (red) and their overlay in tumor tissues from MC38 tumors. **C**. Kaplan-Meier survival curves comparing the high and low expression of CXCR6 in breast, liver, lung and gastric cancer analyzed by Kaplan-Meier Plotter Database (https://kmplot.com/analysis/). **D**. Survival curve comparing the high and low expression of CXCR6 in skin cutaneous melanoma (SKCM) analyzed by GEPIA website. **E and F**. Representative plots $CXCR6^{+}CD8^{+}$ T cells in peripheral blood (PB), lymph node (LN), spleen and tumor from CT26 tumor-bearing mice. **H**. The expression of CXCR6 on NK cells in MC38 tumor tissue. **G**. Gating strategy for determination of CXCR6 expression on tumor-infiltrating $CD8^{+}$ T cells. ***$P< 0.001$.

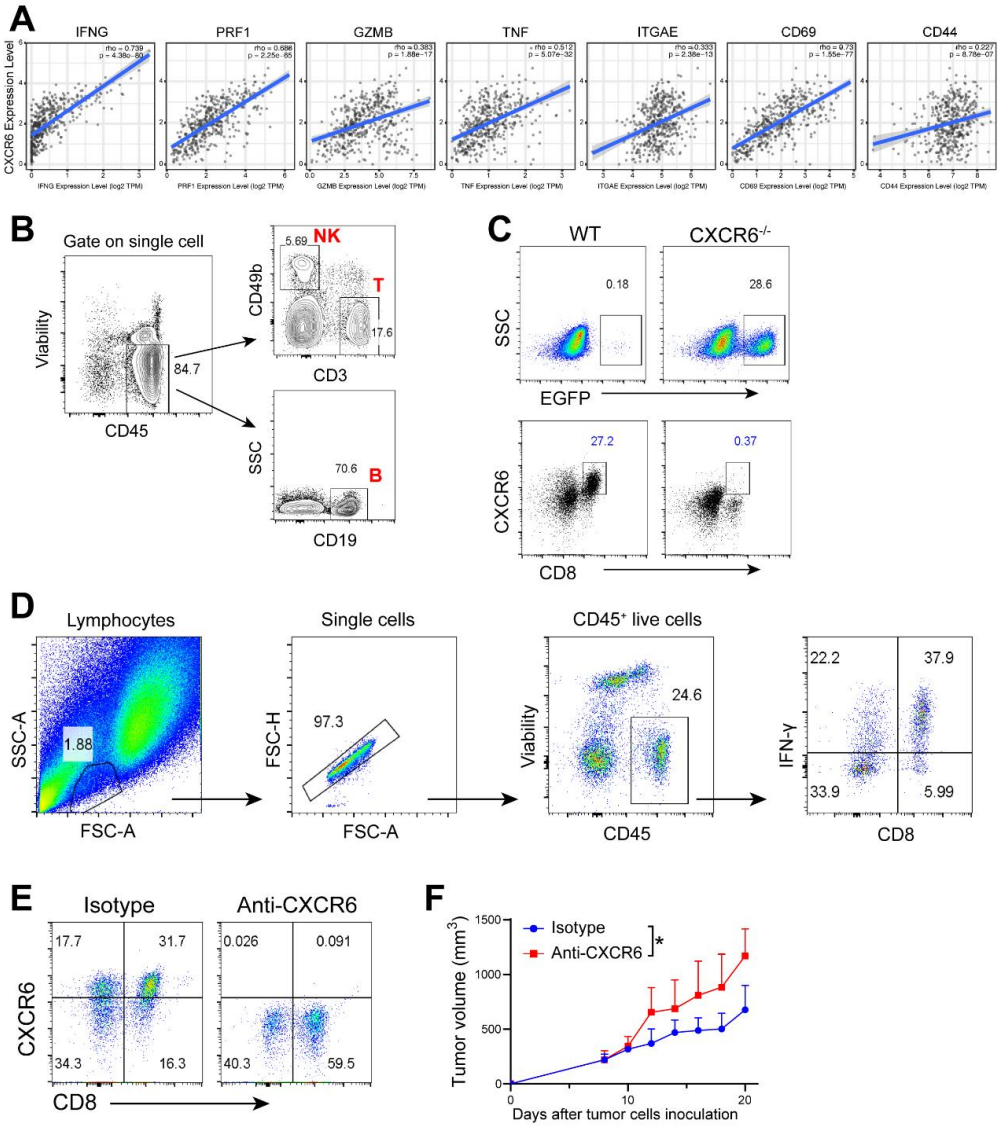

Figure S2. Chimeras with *Cxcr6* deficiency on CD8⁺ T cell are reconstituted successfully.

A. Scatterplots showing correlation between CXCR6 and IFNG, PRF1, GZMB, TNF, ITGAE, CD69, CD44 expression in COAD in TCGA database determined by Tumor Immune Estimation Resource (TIMER, http://cistrome.dfci.harvard.edu/TIMER/) website. **B.** Dot plots showing the proportions of T, B and NK cells in chimeras. **C**. Identification of knockout mice with deletion of *Cxcr6*. **D**. Gating strategy for figure 2I. **E**. Identification of efficacy of anti-CXCR6. **F**. Tumor growth (n = 8). **P*< 0.001.

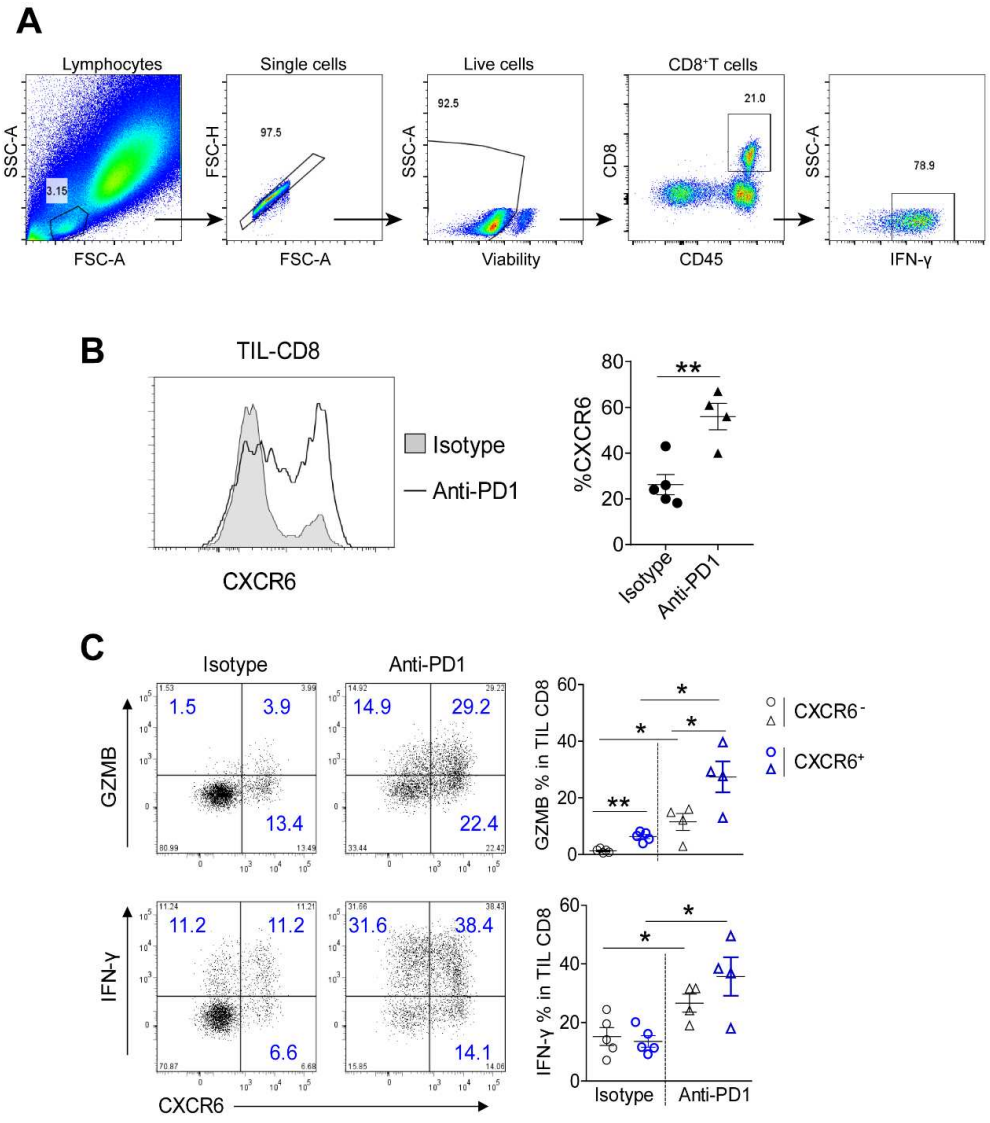

Figure S3. CXCR6⁺CD8⁺ T cells respond anti-PD-1 treatment more effectively in melanoma.

A. Gating strategy for figure 3E. **B and C.** Proportions of tumor-infiltrating CD8⁺ T cells (**B**) and effectors produced (**C**) was quantified from mice treated with isotype or anti-PD-1. Data are presented as the mean ± SEM. **P* < 0.05, ***P* < 0.01. Statistical significance determined by two-way ANOVA with Tukey's multiple comparison test.

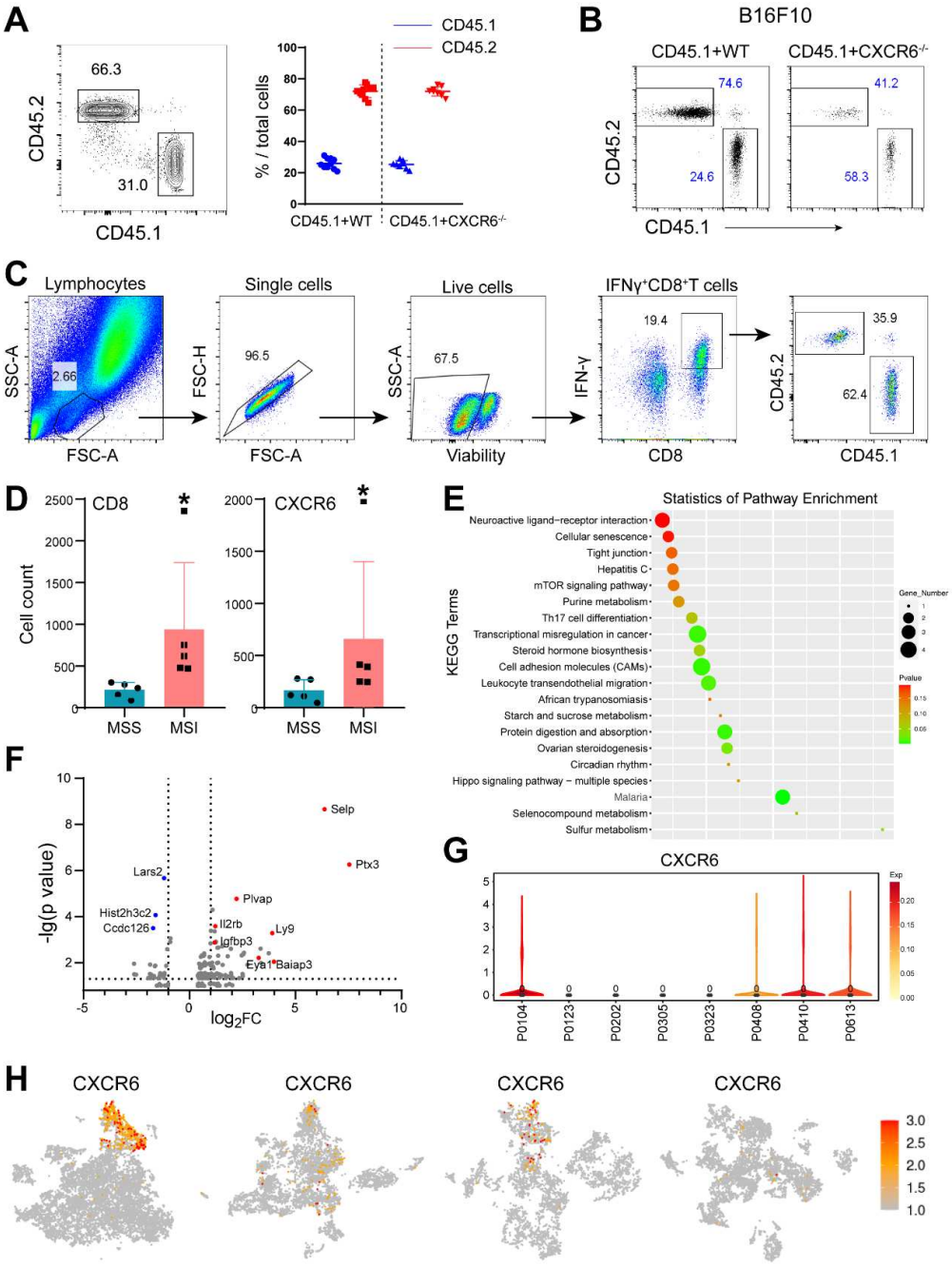

Figure S4. Chimeras with CD45.1 and CD45.2 double positive are reconstituted successfully.

A. Dot plots showing the proportions of $CD45.1^+$ and $CD45.2^+$ cells from PB in chimeras. **B**. Quantification of $CD45.1^+$ and $CD45.2^+$ cells from melanoma gated on $CXCR6^+CD8^+$ cells in chimeras. **C**. Gating strategy for figure 4C. **D**. Statistics for figure 4D. **E**. KEGG enrichment of top 20 pathways. **F**. Volcanoplot of selected genes. **G**. Violin plot showing the expression of CXCR6 from colon cancer

patients reported previously (Zhang L, et al. Cell. 2020). **H**. t-SNE plots showing CXCR6 expression in for 4 colon cancer patients. Single cell RNA sequencing data was from our previous dataset (unpublished).

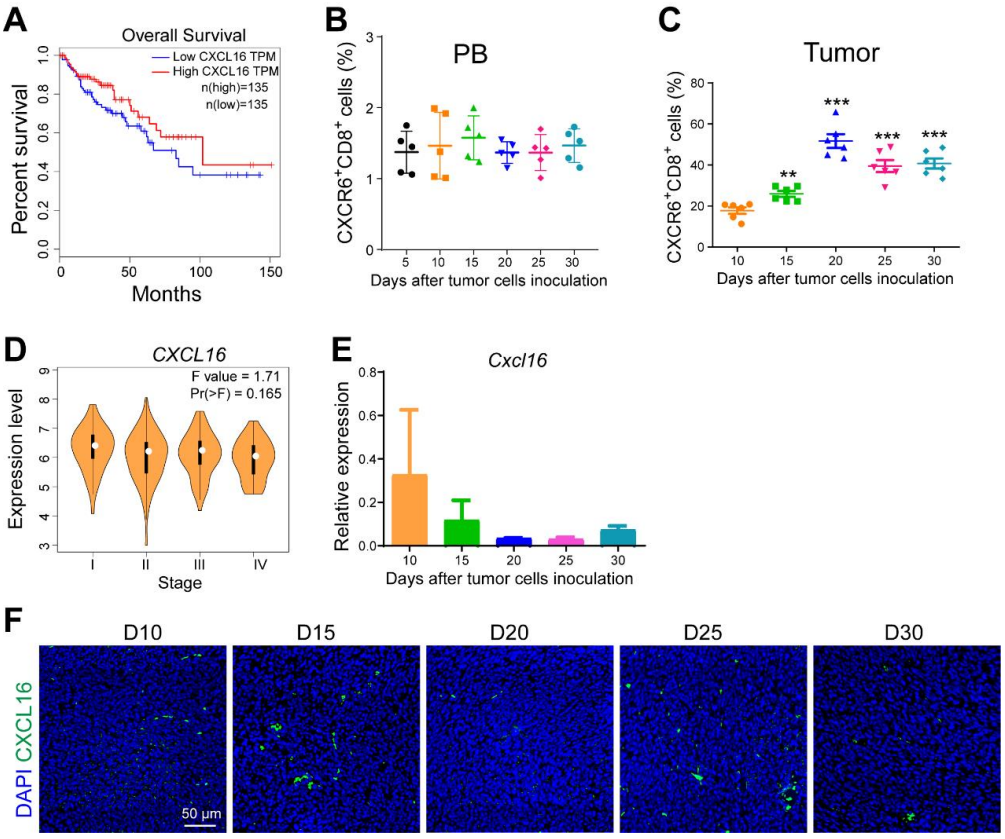

Figure S5. The changes of CXCR6 and CXCL16 are not synchronous.

A. Survival curve comparing the high and low expression of CXCR6 in COAD analyzed by GEPIA website. **B and C**. Timing course of proportions of $CXCR6^{+}CD8^{+}$ T cells in PB (**B**) and tumor (**C**) from tumor burden mice. **D**. The mRNA expression level of CXCL16 across tumor stages from patients in TCGA database. **E**. Relative gene expression of Cxcl16 on different days after tumor cells inoculation in murine MC38 xenograft model. **F**. Immunofluorescence staining showing DAPI (blue) / CXCL16 (green) in tumor tissues from murine MC38 xenograft model. Data are presented as the mean ± SEM. $^{**}P < 0.01$, $^{***}P < 0.001$. Statistical significance determined by two-way ANOVA with Tukey's multiple comparison test.

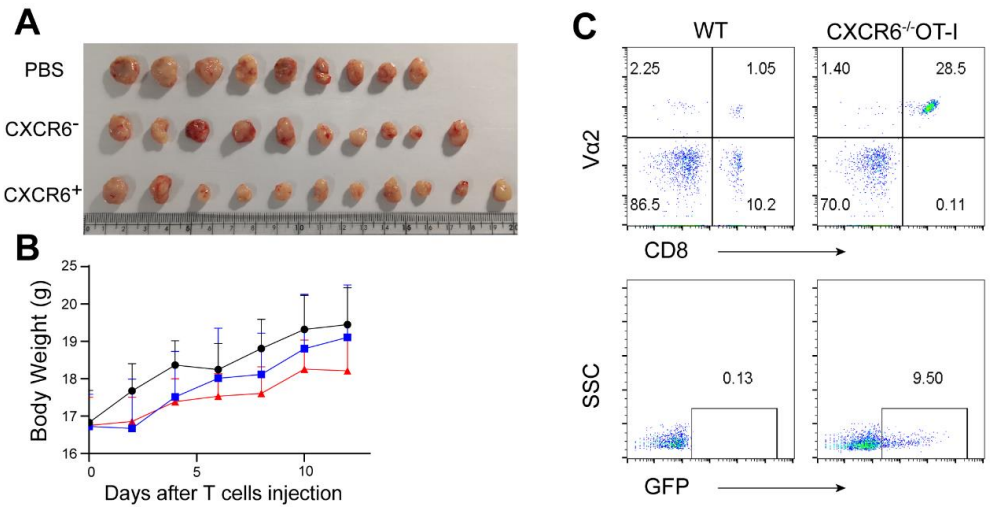

Figure S6. CXCR6$^{-/-}$ OT-I mouse are constructed successfully.

A. Images of tumors. **B**. Body weight curves. **C**. Dot plots showing identification of the second generation of intercrossed mice including *Cxcr6*$^{-/-}$and OT-I strains.